

# THERMAL DEGRADATION OF POLYIMIDE INSULATION AND ITS EFFECT ON ELECTROMAGNETIC COIL IMPEDANCE

N. Jordan Jameson, Michael H. Azarian, and Michael Pecht  
Center for Advanced Life Cycle Engineering (CALCE)  
Building 89, Room 1100C  
University of Maryland, College Park, MD 20742  
Telephone: (301) 405-8038  
jjameson@umd.edu

**Abstract:** The failure of insulation in electromagnetic coils is a significant cause of coil failure and can have severe implications for the system in which the coil is used. Impedance monitoring of coils has emerged as a promising avenue for evaluating the insulation health of electromagnetic coils in-situ. Due to its excellent mechanical properties and ability to endure high temperatures, polyimide is widely used as an insulator in the electromagnetic coil manufacturing industry. However, little information is known about the electrical behavior of polyimide insulation when subjected to the variety of stresses experienced when used as electromagnetic coil insulation, casting uncertainty on the use of impedance monitoring when monitoring polyimide insulation health. This paper presents an experimental analysis of how the insulation electrical parameters evolve over time, and their consequent effect on the coil impedance spectrum, thus providing useful empirical evidence for impedance monitoring for electromagnetic coil insulation health monitoring.

**Keywords:** Condition monitoring, electromagnetic coil insulation, insulation health monitoring, impedance measurement, insulation capacitance, insulation resistance, polyimide thermal degradation

**Introduction:** Electromagnetic coils are used ubiquitously in a variety of industries and industrial applications, including electric motors, solenoid valves, and transformers. Studies have shown that between one-quarter [1], [2] and one-third [3] of motor failures are due to failures in the insulation. A study of U.S. nuclear power plants [4] showed that over 50% of solenoid valve failures originated with failures in the electromagnetic coil (e.g., coil opens or coil shorts).

There has been much work addressing the problem of insulation health monitoring in machinery. In 2004, Stone *et al.* [5] released a book that is a standard reference for insulation used in rotating machinery. In it, the available methods of diagnostics for insulation were discussed. For in-situ insulation health monitoring, the available methods are partial discharge testing or particulate measurement (i.e., smoke detector) [6], [7]. However, many machines, such as low-voltage motors or solenoid-operated valves, operate at voltages that do not induce partial discharge (or induce such low levels as to be unmeasurable). Offline methods include the measurement of the dissipation factor,

insulation capacitance, polarization index, insulation resistance, insulation power factor, and offline partial discharge. A common theme for the offline methods discussed is direct access to the insulation. In other words, in order to measure the insulation capacitance, for example, one must have the ability to place electrodes outside the insulation, in effect using the insulation as a dielectric between the inner conductor and the outer electrodes. This is not practical for most coils, since measurement of these parameters requires disassembly of the system in which the coil is used. Hence, it is necessary to find a method that can detect insulation degradation and does not rely on these traditional methods.

Early efforts at using coil terminal impedance as an insulation health monitoring feature were outlined in patents from Kendig and Rogovin [8], [9]. The authors did not disclose any quantitative analyses of their proposal, nor did they publish any technical papers; it was an idea without a technical foundation. In 2006, Werynski *et al.* [10] asserted that the impedance resonant frequency could be used as a feature for coil insulation health monitoring. Their work was followed in 2007 and 2009 by Perisse *et al.* [11], [12], and in 2013 by Savin *et al.* [13]. These studies showed that changes in the insulation capacitance cause increases in impedance resonant frequency. The drawbacks of their work are as follows. First, the aging processes were based upon a uniform temperature in the coil since the coils were aged in a high temperature oven. Second, insulation resistance was not studied, but Younsi *et al.* [14] showed that insulation resistance can play a significant role in understanding the aging condition of electromagnetic coil insulation.

Polyimide, a common insulation material used in electromagnetic coils, is a polymer constructed of imide monomers, which consist of two acyl groups bound to a nitrogen. The chemical structure of “Kapton”, a classic polyimide, is shown in Figure 1. The high resistance of polyimide to thermal degradation and its high mechanical strength leads to diverse applications including high temperature fuel cells, liquid crystal alignments, and magnet wire insulation for use in electromagnetic coils [15], [16]. Polyimide insulation is given a 240 °C temperature rating, which means that the insulation is expected to survive for 20,000 hours (about 2.3 years) at 240 °C before experiencing electrical breakdown, according to ASTM D2307 [17]. Previous studies of polyimide aging [18]–[20] only examined films ( $1.5 < \text{thickness} < 125 \mu\text{m}$ ) of polyimide under various degradation mechanisms (thermal, radiation, saline exposure). The results from these studies are mixed and inconsistent. Further, none of these studies examined the mechanical stresses that would be present when polyimide is applied as an electromagnetic coil insulator (due to Joule heating and the resulting expansion of the conductor). Moreover, the ASTM standard does not address the mechanical stress that the magnet wire will experience when applied in electromagnetic coils.

In this paper, dual-wound coils constructed using polyimide insulation are aged using Joule heating effects from applied power, which is a more realistic aging condition than the uniform temperature aging provided by an oven. Further, the coil impedance, the insulation impedance, and the insulation resistance are measured to provide insight into the aging process of polyimide insulation. The experiments provide data and features that can be incorporated into electromagnetic coil insulation health monitoring schemes.

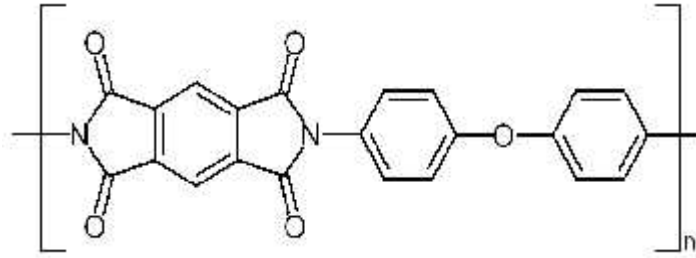


Figure 1: Chemical structure of “Kapton” polyimide

**Experimental Setup:** Dual-wound electromagnetic coils were manufactured by Magnecomp, Inc. (South Carolina, USA), as shown in Figure 2 (a). The parallel magnet wires were wound on a rectangular Pyroglass bobbin. An example of this winding arrangement (though not a replica of the arrangement of the experimental coils) is illustrated in Figure 2 (b), where the base numbers indicate the turn number and the superscript numbers indicate the two parallel windings of magnet wire. Each winding had 230 turns of AWG 27 (conductor diameter of  $361 \mu\text{m} \pm 3 \mu\text{m}$ ) of Heavy Alex® polyimide insulation. This produced 7 layers of parallel windings, and each winding had a DC resistance of about  $2.44 \Omega$ .



Figure 2: Dual-wound coil (a) received units; and (b) winding arrangement illustration.

In order to age the insulation in a manner closely resembling the stresses that would be likely in an application condition, one of the parallel windings was powered to produce an average internal temperature of  $200 \text{ }^\circ\text{C}$ . This temperature was determined using the temperature-resistance relationship as shown in (1), where  $\alpha = 0.00393/^\circ\text{C}$  for copper, and  $R_0$  and  $T_0$  are reference resistance and temperature, respectively. The final average temperature of the coil is given by  $T(R_T)$  and the final resistance is given by  $R_T$ . Generally, the required voltage was between 7.7 and 7.8 V, and after the transient behavior settled, the current was between 1.8 and 1.85 A.

$$T(R_T) = \frac{1}{\alpha} \left( \frac{R_T}{R_0} + \alpha T_0 - 1 \right) \quad (1)$$

The coils were removed from the power periodically and three measurements were performed. First, the terminal impedance of one of the windings was measured using an

Agilent E4980A LCR meter at 501 distinct frequencies over the frequency range  $f \in [20, 2e6]$  Hz with a 500 mV rms signal. This is illustrated for a single winding in Figure 3 (a). Second, the impedance of the insulation was measured using an Agilent E4980A LCR meter at 201 distinct frequencies in the frequency range  $f \in [20, 2e6]$  Hz with a 1 V rms signal. This measurement was performed by shorting the terminals of each winding as illustrated in Figure 3 (b), which allowed the electric field to be directed through the insulation only. Third, the response of the insulation to a step application of 100 V was measured, allowing for measurement of DC resistance characteristics of the insulation. This measurement was performed with the coil windings in the same setup as for the insulation impedance. For this measurement, a 100 VDC potential was placed across the insulation and held for 20 minutes, while the current was sampled once per second.

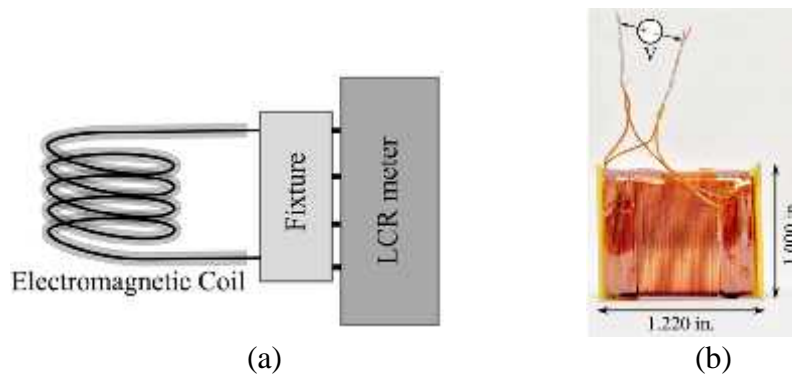


Figure 3: Measurement setup for (a) winding terminal impedance; and (b) insulation impedance and resistance.

**Experimental Results:** Impedance is a complex-valued variable, which means it can be represented in polar form,  $Z = |Z|e^{j\theta}$ , or Cartesian form,  $Z = \Re\{Z\} + j\Im\{Z\} = R + jX$ , where  $j = \sqrt{-1}$ . In Cartesian form, the real part is referred to as resistance (not to be confused with DC resistance), and the imaginary part is referred to as reactance. Reactance, the imaginary part of impedance, can be further broken into inductive reactance,  $X_L = \omega L$ , and capacitive reactance,  $X_C = -(\omega C)^{-1}$ , such that  $X = \Im\{Z\} = X_L + X_C$ , where  $\omega = 2\pi f$  is angular frequency in rad/s (and  $f$  is frequency in Hz). Since any given reactance measurement is either positive or negative, when  $X > 0$ , the total reactance is said to be inductive, and when  $X < 0$ , the total reactance is said to be capacitive. The impedance spectra, shown in Cartesian form, for the one of the windings over 1103 hours of aging is shown in Figure 4. The resulting increase in the resonant frequency (the frequency where reactance crosses zero) was reproduced in the other samples.

The insulation impedance measurements can also be split into real and imaginary parts. In these measurements, reactance was negative (capacitive) over the entire frequency range,  $f \in [20, 2e6]$  Hz. Therefore, each reactance measurement was converted into capacitance using the relationship  $C = -(\omega X_C)^{-1}$ . As can be seen in Figure 5, the insulation capacitance (at 100 kHz) decreased over the aging period. This behavior was replicated in all three samples. It must be noted that the samples aging period was limited

by the life of the terminals. Since the terminals are made of magnet wire, the mechanical stresses introduced by bending caused the terminals to fail prior to the polyimide insulation. Nevertheless, the aging trend of the insulation is clear and repeatable over the three samples shown. In one of the samples, there is an increase in the capacitance between about 450 hours and 620 hours. This is a partial recovery after the coil was removed from thermal stress for 1 week. Hence, the insulation degradation process, as reflected in the electrical parameter measurement, is at least partially reversible. However, after being reconnected to power, the capacitance not only returned to its previous value, but the trend continued downward.

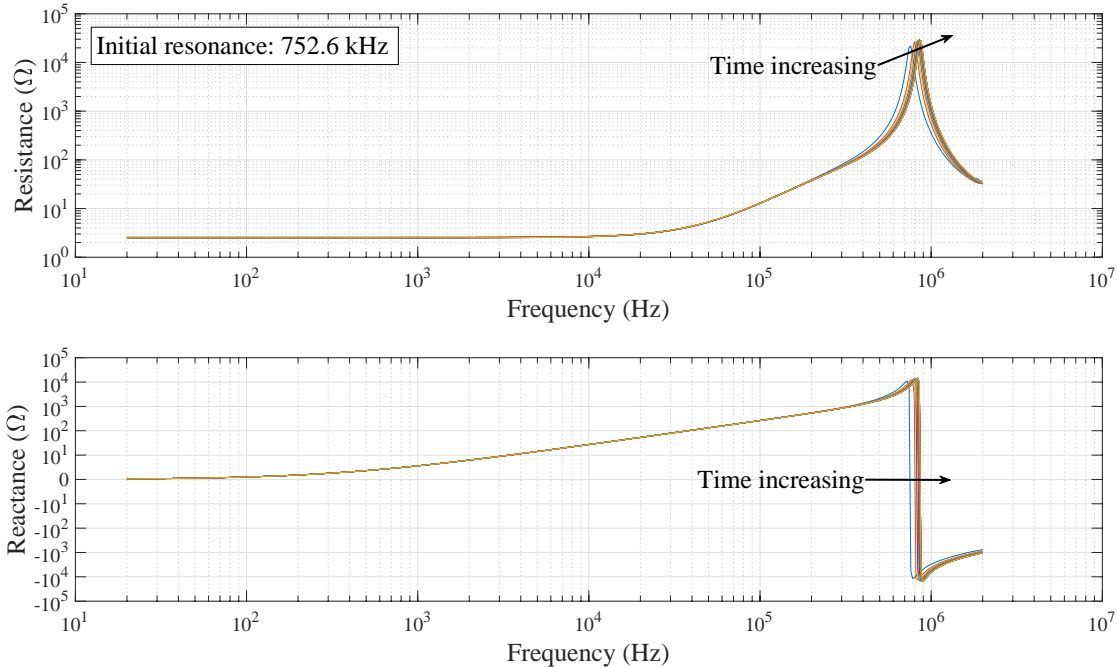


Figure 4: Resistance (above) and reactance (below) spectra of one coil winding over the course of an experiment (1172 hours).

The analysis of the insulation current was performed as follows. First, the insulation current of healthy insulation was measured over an extended period of time, in order to allow the current to settle. This was done by placing 100 VDC across the insulation, and measuring the resulting current. The initial insulation current measurements for two coils are shown in Figure 6. One coil was measured for about 8.3 hours with current measurements taken every 3 seconds and the other for 13.8 hours with current measurements taken every 5 seconds. Then, in order to measure the effect of aging on the insulation resistance, the current was sampled every 1 second for 20 minutes. These results are shown in Figure 7 and Figure 8. (For the insulation current measurements, only two samples were available due to experimental complications.)

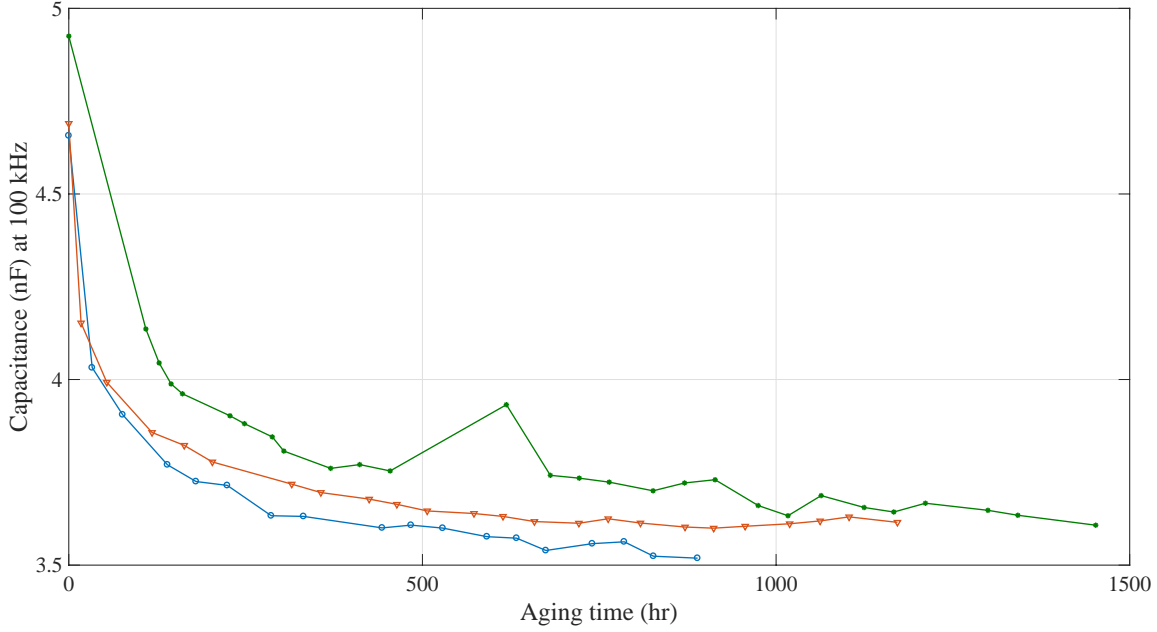


Figure 5: Change in polyimide insulation capacitance as a result of thermal aging at an average coil temperature of 200 °C. The line colors and markers correspond to three different coils.

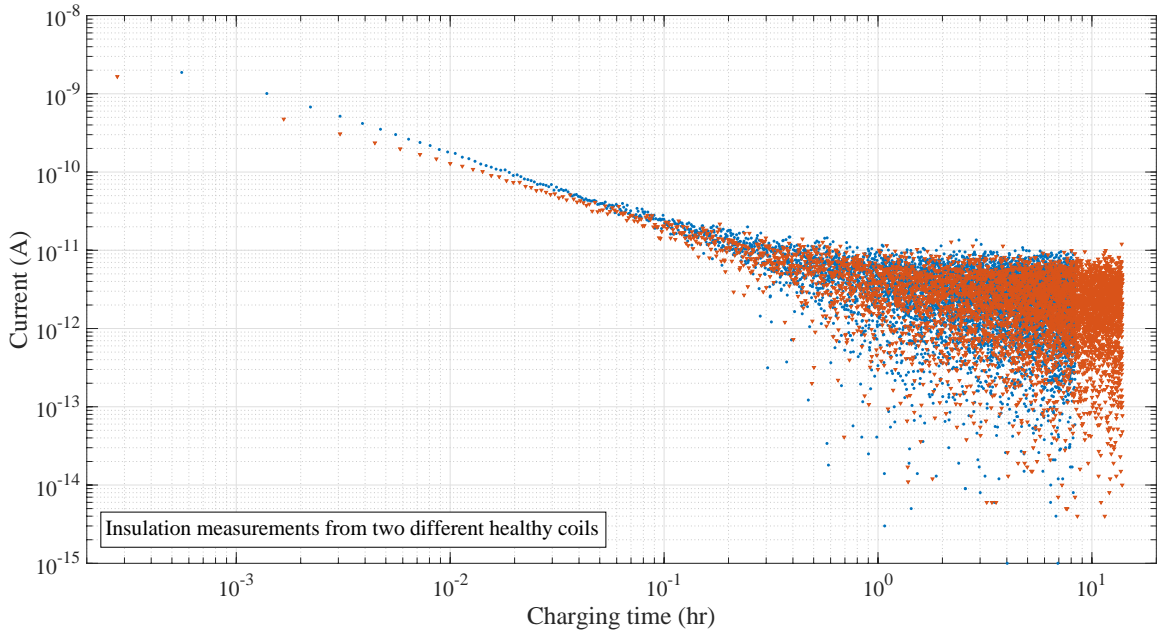


Figure 6: Polyimide insulation current measurements for new (healthy) insulation. The two colors and markers represent two different coils.

The relationship between the polarization current and the charging time can be expressed using the Curie-von Schweidler “universal law” for dielectrics [21]–[25] as shown in (2), where  $\bar{i}_p(t_c)$  is the polarization current at charging time,  $t_c$ , and  $0 < n < 1$  is the power law exponent.

$$i_p(t_c) \propto t_c^{-n} \quad (2)$$

The curves shown in Figure 6 clearly show this behavior, with the current settling to a constant value such that the total current is as expressed in (3).

$$i_p(t_c) = at_c^b + c \quad (3)$$

In (3),  $a$  is the coefficient of proportionality,  $c$  is the steady-state (or conduction) current, and  $-1 < b < 0$  is the power law decay of the polarization current. The curve (3) can be fit to the data using a robust non-linear least squares algorithm. The robustness in the algorithm ensures that the adjustments to the function are less sensitive to outliers in the data. In this work, the least absolute residual (LAR) method for robust regression was used, which minimizes the absolute value of the residual instead of minimizing the square of the residual. Therefore, the extreme values have a lesser influence on the fit. Some insulation current measurements are shown in Figure 7. The measurement procedure was altered after the first two measurements to begin the current measurements at 1 second as opposed to 3 seconds. This is the reason for the difference in the starting times for the data.

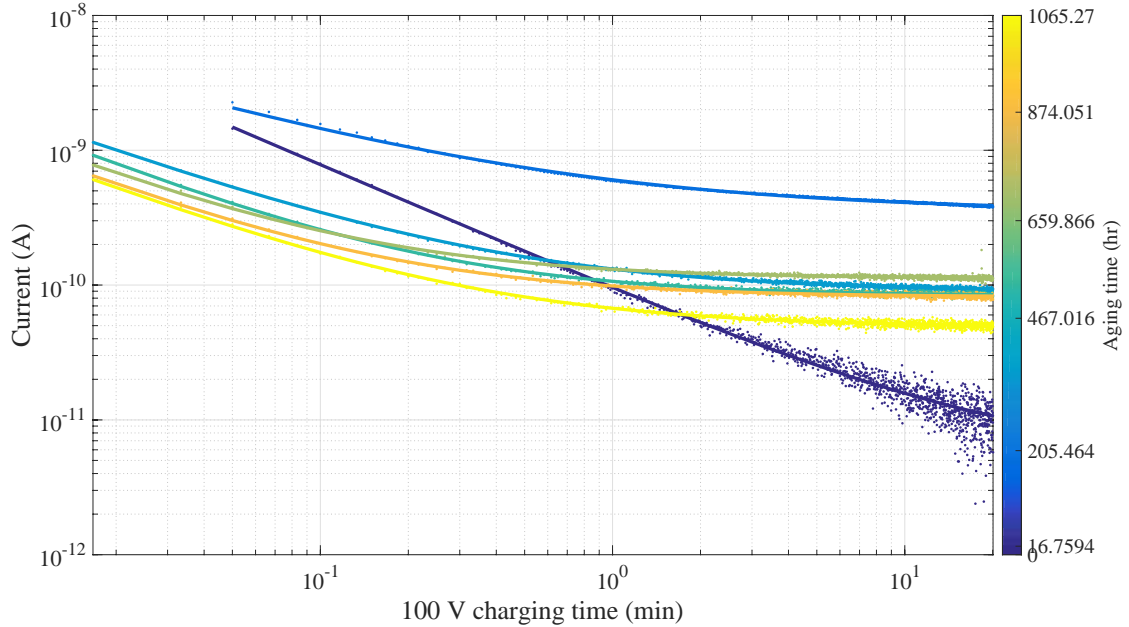


Figure 7: Measurements of insulation current versus charging time at 100 VDC as the insulation aged at an average coil temperature of 200 °C. The lines are drawn over the data and are shown in the same color as the raw data.

It is clear that as the insulation is aged, the insulation resistance changes. In fact, from the first measurement to 16.76 hours of aging, there is a significant decrease in the insulation resistance. In order to illustrate how the insulation resistance changed for two samples as the insulation aged, the regression fit parameters are shown in Figure 8. The data appears to be agree between the two samples for the parameters  $a(t)$  and  $c(t)$ , whereas there are

large differences in the parameter  $b(t)$  between the two samples. The values of  $c(t)$  show that the conduction current of the insulation increased over the aging period, or equivalently, the resistance of the insulation decreased as the insulation aged.

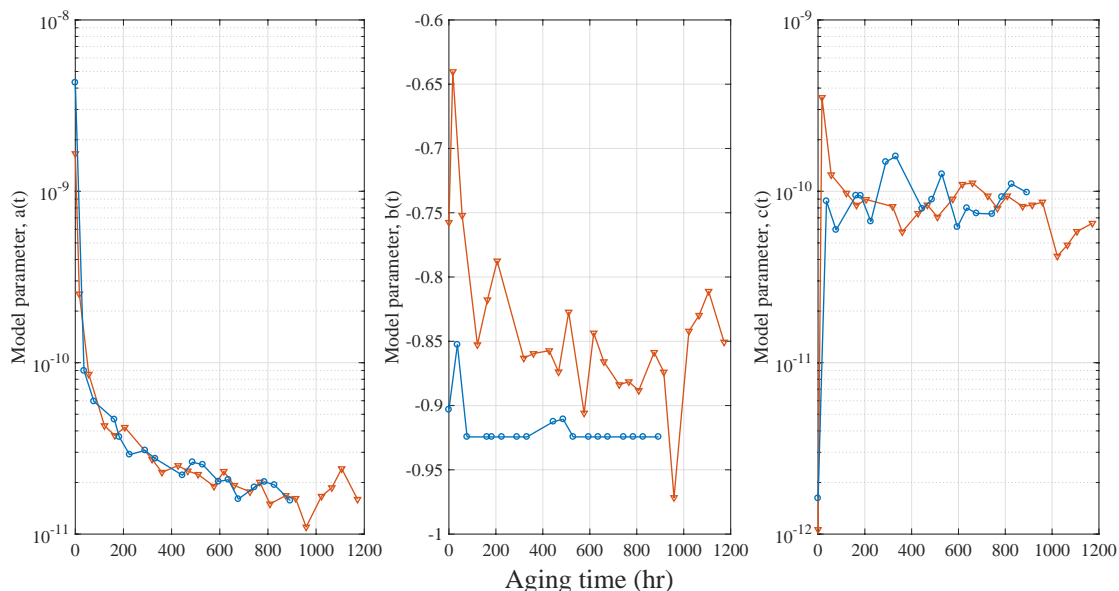


Figure 8: Evolution of regression fit of the polarization current as the insulation aged at an average coil temperature of 200 °C. The marker styles and colors correspond to two different coils.

**Terminal impedance data analysis:** Previous work [26]–[28] showed that not only do terminal impedance measurements capture changes in the insulation, but there are frequencies within the impedance spectrum that capture the insulation degradation information better than others. To explore this effect in the coils studied in this paper, a Spearman correlation spectrum was constructed. The Spearman correlation coefficient for  $n$  samples,  $X_i, Y_i$  is computed by first converting the raw data into ranked variables  $x_i$  and  $y_i$ , then forming the distance measure  $d_i = y_i - x_i$ .

$$\rho_S = 1 - \frac{6}{n(n^2 - 1)} \sum_{i=1}^n d_i^2 \quad (4)$$

The Spearman correlation coefficient is a measure of linear and nonlinear monotonic correlation [29], and hence, is more general than Pearson correlation, which only measures linear correlation. The Spearman correlation coefficient was computed using the vector of time entries when the coil was removed from power and measured, and the time series of each impedance measurements at each frequency. This resulted in a vector that is the same length as the number of frequencies,  $N = 501$ , where each entry is a Spearman correlation coefficient quantifying the degree of monotonicity of any given impedance measurement at a particular frequency over the degradation time period. Thus, the impedance at each frequency is assessed as a potential health indicator independently of the other frequencies.

The Spearman correlation spectra show the differences in behavior of resistance ( $\Re\{Z\}$ ) and reactance ( $\Im\{Z\}$ ) as the coils aged. In general, there is significant agreement among the reactance Spearman spectra, with root mean square (RMS) difference values of 0.0905, 0.1052, and 0.0941 between the three curves. The resistance Spearman spectra have much larger RMS difference values of 0.6898, 0.3589, and 0.7331 between the three curves.

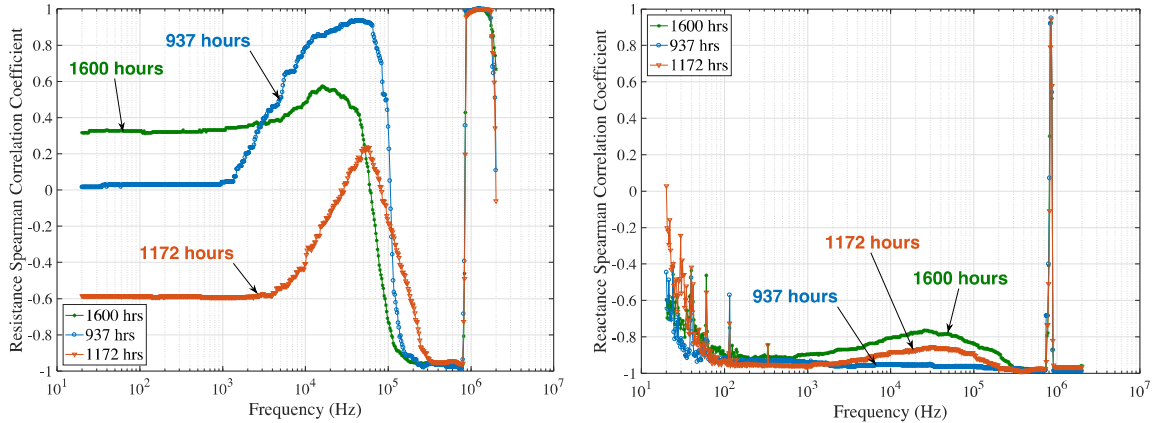


Figure 9: Resistance (left) and reactance (right) Spearman correlation spectrum for 3 coil samples aged at an average coil temperature of 200 °C. The line colors and markers correspond to three different coils aged for different lengths of time.

Consider the time series of reactance at  $f = 604$  kHz (one of the minimum points in the three reactance Spearman spectra) and  $f = 853.2$  kHz (the maxima of the three reactance Spearman spectra) as shown in Figure 10. The “recovery” in one of the coils (as mentioned with the capacitance measurements) is visible between 450 and 620 hours. Similarly, consider the resistance (i.e.,  $\Re\{Z\}$ ) at  $f = 778.1$  kHz and  $f = 1.262$  MHz as shown in Figure 11.

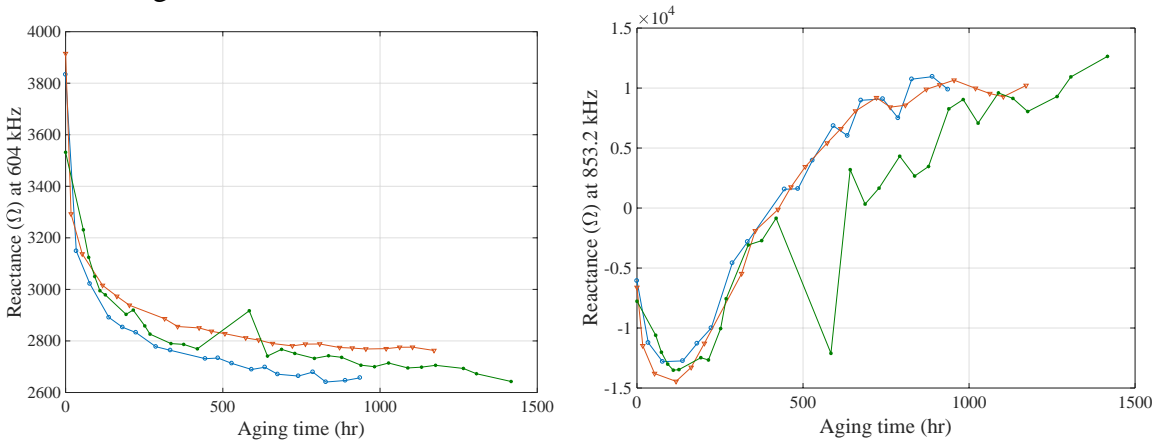


Figure 10: Change in reactance at  $f = 604$  kHz (left) and  $f = 853.2$  kHz (right) over the aging period for three coils. The line colors and markers correspond to three different coils.

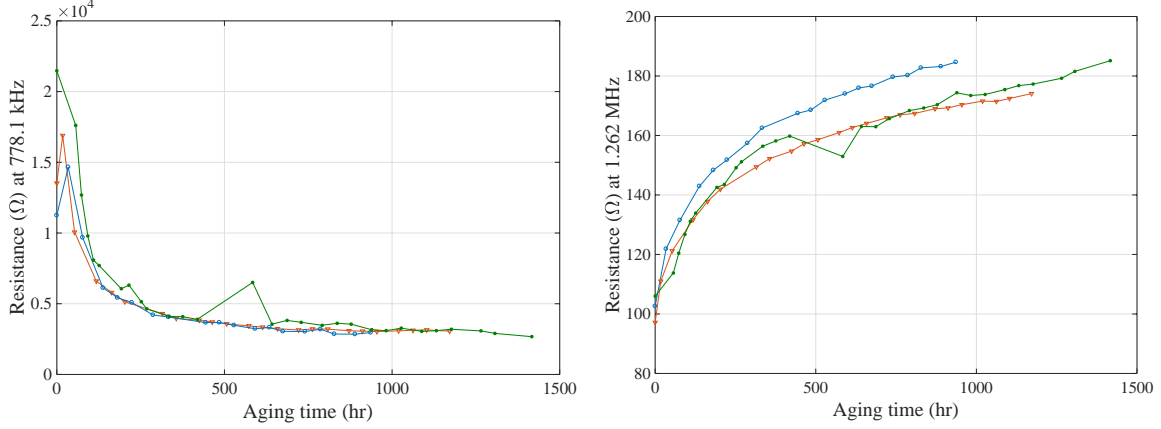


Figure 11: Change in reactance at  $f = 778.1$  kHz (left) and  $f = 1.262$  MHz (right) over the aging period for three coils. The line colors and markers correspond to three different coils.

Table 1: Percent changes in relevant frequencies for resistance and reactance, and the changes in the resonant frequency for all three coils.

Frequency	Percent change: $\% \text{ change} =  (x_c - x_f)/x_c  \times 100\%$		
	Resistance, $R = \{Z\}$	Reactance, $X = \{Z\}$	Resonant frequency
778.1 kHz	73.65, 77.20, 85.59	*	*
1.262 MHz	79.93, 76.57, 66.75	*	*
604 kHz	*	30.69, 29.43, 23.60	*
853.2 kHz	*	263.1, 254.3, 217.7	*
*	*	*	15.60, 14.89, 13.30

The data shown in Table 1 demonstrates the relative sensitivity of frequencies below and above the coil resonant frequency to changes in the electrical properties of the insulation. Further, the trends are repeatable across three samples. Not all coils (with various geometries and insulation materials) experience the same amount of migration of the resonant frequency with aging. It is therefore necessary to observe the most sensitive feature, which is shown not to be the resonant frequency, contrasting with suggestions in [10]–[12].

**Conclusion:** The degradation of insulation in electromagnetic coils can result in failure of the coil, which in turn can result in the failure of the system using the coil. Past studies have shown insulation failure to be a significant cause of failure in electric motors and solenoid valves.

This paper investigated the changes in the electrical behavior of polyimide insulation while being aged at an average coil temperature of 200 °C. Polyimide is a widely-used insulation with high resistance to thermal degradation (rated for 240 °C) and high mechanical strength. The study presented herein showed that as polyimide insulation aged, the coil resonant frequency increased, the capacitance dropped, and the steady-state DC resistance of the insulation decreased. This data can be used to understand the

thermal degradation nature of polyimide and to design impedance-based health monitoring systems for electromagnetic coils that use polyimide insulation.

The terminal impedance data was analyzed showing that within the impedance spectrum, there are frequencies that are very sensitive to changes in the electrical properties of the insulation. Four frequencies were given that had percent changes between 2 and 16 times larger than that experienced by the resonant frequency. This provides further experimental support to the hypothesis presented in [26] and [27]. Moreover, a Spearman correlation spectrum provided a holistic view of the changes in the impedance spectra as the coils aged, which can be related to the changes in the insulation electrical parameters. In other words, the decreasing insulation capacitance and insulation resistance resulted in the observed changes in the impedance spectrum as the coils aged. In knowing the relationship between these variables, a suitable threshold can be established, allowing for condition-based maintenance to be properly implemented.

**Acknowledgement:** The authors would like to thank Magnecomp, Inc. for generously donating the coils used in the presented experiments. Further thanks go to the more than 100 companies that sponsor research activities at the Center for Advanced Life Cycle Engineering (CALCE) at the University of Maryland annually.

#### References:

- [1] Motor Reliability Working Group, "Report of large motor reliability survey of industrial and commercial installations, Part I," *IEEE Trans. Ind. Appl.*, vol. IA-21, no. 4, pp. 853–864, Jul. 1985.
- [2] Motor Reliability Working Group, "Report of large motor reliability survey of industrial and commercial installations, Part II," *IEEE Trans. Ind. Appl.*, vol. IA-21, no. 4, pp. 865–872, Jul. 1985.
- [3] O. V. Thorsen and M. Dalva, "A survey of faults on induction motors in offshore oil industry, petrochemical industry, gas terminals, and oil refineries," *IEEE Trans. Ind. Appl.*, vol. 31, no. 5, pp. 1186–1196, Sep. 1995.
- [4] V. P. Bacanskas, G. C. Roberts, and G. J. Toman, "Aging and service wear of solenoid-operated valves used in safety systems of nuclear power plants. Volume 1: Operating experience and failure identification," Oak Ridge National Laboratory, Mar. 1987.
- [5] G. C. Stone, E. A. Boulter, I. Culbert, and H. Dhirani, *Electrical Insulation for Rotating Machines: Design, Evaluation, Aging, Testing, and Repair*. John Wiley, 2004.
- [6] S. Grubic, J. M. Aller, B. Lu, and T. G. Habetler, "A survey on testing and monitoring methods for stator insulation systems of low-voltage induction machines focusing on turn insulation problems," *IEEE Trans. Ind. Electron.*, vol. 55, no. 12, pp. 4127–4136, Dec. 2008.
- [7] P. J. Tavner, "Review of condition monitoring of rotating electrical machines," *IET Electr. Power Appl.*, vol. 2, no. 4, pp. 215–247, 2008.

- [8] M. W. Kendig and D. N. Rogovin, "Method of conducting broadband impedance response tests to predict stator winding failure," U.S. Patent 6 323 658 B1, 27-Nov-2001.
- [9] M. W. Kendig and D. N. Rogovin, "Method of conducting broadband impedance response tests to predict stator winding failure," U.S. Patent 6 483 319 B1, 19-Nov-2002.
- [10] P. Werynski, D. Roger, R. Corton, and J.-F. Brudny, "Proposition of a new method for in-service monitoring of the aging of stator winding insulation in AC motors," *IEEE Trans. Energy Convers.*, vol. 21, no. 3, pp. 673–681, Sep. 2006.
- [11] F. Perisse, D. Mercier, E. Lefevre, and D. Roger, "Robust diagnostics of stator insulation based on high frequency resonances measurements," *IEEE Trans. Dielectr. Electr. Insul.*, vol. 16, no. 5, pp. 1496–1502, Oct. 2009.
- [12] F. Perisse, P. Werynski, and D. Roger, "A new method for AC machine turn insulation diagnostic based on high frequency resonances," *IEEE Trans. Dielectr. Electr. Insul.*, vol. 14, no. 5, pp. 1308–1315, Oct. 2007.
- [13] S. Savin, S. Ait-Amar, and D. Roger, "Organic enameled wire aging monitoring based on impedance spectrum analysis," in *2012 Annual Report Conference on Electrical Insulation and Dielectric Phenomena (CEIDP)*, 2012, pp. 874–877.
- [14] K. Younsi, P. Neti, M. Shah, J. Y. Zhou, J. Krahn, K. Weeber, *et al.*, "On-line capacitance and dissipation factor monitoring of AC stator insulation," *IEEE Trans. Dielectr. Electr. Insul.*, vol. 17, no. 5, pp. 1441–1452, Oct. 2010.
- [15] D.-J. Liaw, K.-L. Wang, Y.-C. Huang, K.-R. Lee, J.-Y. Lai, and C.-S. Ha, "Advanced polyimide materials: Syntheses, physical properties and applications," *Prog. Polym. Sci.*, vol. 37, no. 7, pp. 907–974, Jul. 2012.
- [16] A. Georgiev, D. Dimov, E. Spassova, J. Assa, P. Dineff, and G. Danev, "Chemical and Physical Properties of Polyimides: Biomedical and Engineering Applications," in *High Performance Polymers - Polyimides Based - From Chemistry to Applications*, M. J. M. Abadie, Ed. InTech, 2012.
- [17] "D2307 – 07a: Standard Test Method for Thermal Endurance of Film-Insulated Round Magnet Wire." ASTM International, 2013.
- [18] L. Li, N. Bowler, P. R. Hondred, and M. R. Kessler, "Dielectric response of polyimide to thermal and saline degradation," in *2010 Annual Report Conference on Electrical Insulation and Dielectric Phenomena (CEIDP)*, 2010, pp. 1–4.
- [19] S. Diahm, M. L. Locatelli, and T. Lebey, "Improvement of Polyimide Electrical Properties During Short-Term of Thermal Aging," in *2008 Annual Report Conference on Electrical Insulation and Dielectric Phenomena*, 2008, pp. 79–82.
- [20] R. Khazaka, M. L. Locatelli, S. Diahm, and P. Bidan, "Effects of mechanical stresses, thickness and atmosphere on aging of polyimide thin films at high temperature," *Polym. Degrad. Stab.*, vol. 98, no. 1, pp. 361–367, Jan. 2013.
- [21] J. Curie, "Recherches sur le pouvoir inducteur spécifique et la conductibilité des corps cristallisés," *Ann. Chim. Phys.*, vol. 17, pp. 385–434.
- [22] E. R. von Schweidler, "Studien über die Anomalien im Verhalten der Dielektrika (Studies on the anomalous behaviour of dielectrics)," *Ann. Phys.*, vol. 329, no. 14, pp. 711–770, Jan. 1907.
- [23] A. K. Jonscher, *Dielectric Relaxation in Solids*. Chelsea Dielectrics Press Limited, 1983.

- [24] A. K. Jonscher, "Dielectric relaxation in solids," *J. Phys. Appl. Phys.*, vol. 32, no. 14, p. R57, 1999.
- [25] "IEEE Recommended Practice for Testing Insulation Resistance of Electric Machinery," *IEEE Std 43-2013 Revis. IEEE Std 43-2000*, pp. 1–37, Mar. 2014.
- [26] N. Jordan Jameson, Michael H. Azarian, and Michael Pecht, "Impedance-based condition monitoring for insulation systems used in low-voltage electromagnetic coils," *IEEE Trans. Ind. Electron.*, vol. PP, no. 99, pp. 1–10, 2017.
- [27] N. Jordan Jameson, Michael H. Azarian, Michael Pecht, Carlos Morillo, and Kai Wang, "Health monitoring of solenoid valve electromagnetic coil insulation under thermal deterioration," in *Proceedings of MFPT 2016/ISA's 62nd IIS*, Dayton, OH, 2016.
- [28] N. Jordan Jameson, Michael H. Azarian, and Michael Pecht, "Impedance-based health monitoring of electromagnetic coil insulation subjected to corrosive deterioration," in *Proceedings of the Annual Conference of the Prognostics and Health Management Society 2016*, Denver, CO, 2016.
- [29] J. L. Myers, A. Well, and R. F. Lorch, *Research Design and Statistical Analysis*. Routledge, 2010.